

1 LHCb highlights

2 Adam Szabelski^{a,*} on behalf of the LHCb collaboration

3 ^aNational Centre for Nuclear Research, Warsaw, Poland

4 E-mail: adam.szabelski@cern.ch

5 The LHCb collaboration has provided many results related to the DISCRETE conference topic. Namely, these concern CP violation in beauty and charm meson decays as well as in baryon decays and searches for lepton flavour violation. This work is focused on some of the latest measurements of the CP violation, listing the following analyses: $\sin 2\beta$ in $B \rightarrow \psi K_S^0$, CKM angle γ measurement's in $B^\pm \rightarrow D^* h^\pm$, $B^\pm \rightarrow DK^*(892)^\pm$ and $B^0 \rightarrow DK^*(892)^0$, search for CPV in $D^+ \rightarrow K^- K^+ \pi^+$, evidence for CPV in baryon decays, and in beauty to charmonium reaction.

Discrete 2024 in Ljubljana

*Speaker

© Copyright owned by the author(s) under the terms of the Creative Commons Attribution-NonCommercial-NoDerivatives 4.0 International License (CC BY-NC-ND 4.0). All rights for text and data mining, AI training, and similar technologies for commercial purposes, are reserved. ISSN 1824-8039. Published by SISSA Medialab.

<https://pos.sissa.it/>

1. The LHCb spectrometer

The LHCb detector [1, 2] is a single-arm spectrometer covering the forward pseudorapidity region, designed for the study of particles containing b or c quarks. Among its elements that are of particular importance is the silicon-strip vertex locator (VELO) surrounding the proton-proton (pp) interaction region that allows c and b hadrons to be identified from their characteristically long flight distance. The tracking system consists of a dipole magnet and sets of tracking stations before and after the magnet, and provides a measurement of the momentum of charged particles. The two ring-imaging Cherenkov detectors (RICH) are able to discriminate between different species of charged hadrons. In addition, a muon system allows for the identification of muons, and a calorimeter system provides electron identification. The online event selection is performed by a trigger, which consisted of a hardware stage, based on information from the calorimeter and muon systems, followed by a software stage, which applies a full event reconstruction. Under these conditions the Run 1 (years 2011-2012 with the center-of-mass energy 7 and 8 TeV and the total luminosity of 3 fb^{-1}) and Run 2 (2015-2018 with 13 TeV and 6 fb^{-1}) data have been taken,

2. Measurement of CP violation in $B^0 \rightarrow \psi(\rightarrow \ell^+\ell^-)K_S^0(\rightarrow \pi^+\pi^-)$ decays

A measurement of CP violation in the interference of B^0 decays with and without mixing entails the measurement of the periodic change of decay-rate differences of initial B^0 and \overline{B}^0 mesons to a common, CP -invariant final state, f , with time. The underlying decay-time-dependent CP asymmetry can be expressed as

$$A_{CP}(t) = \frac{\Gamma(\overline{B}^0(t) \rightarrow f) - \Gamma(B^0(t) \rightarrow f)}{\Gamma(\overline{B}^0(t) \rightarrow f) + \Gamma(B^0(t) \rightarrow f)} \simeq S_f \sin(\Delta m_d t) - C_f \cos(\Delta m_d t), \quad (1)$$

where S_f , C_f are the CP -violation parameters and Δm_d is the $B^0 - \overline{B}^0$ mixing frequency [3]. Moreover, the fact that mixing parameter $\Delta\Gamma_d$ is close to zero is used [4]. The analysis takes into consideration three decay channels of ψ : $J/\psi \rightarrow \mu\mu$, $J/\psi \rightarrow ee$ and $\psi(2S) \rightarrow \mu\mu$. The Run 2 data have been analysed in order to extract the CP -violation parameters resulting in [5]

$$S_{\psi K_S^0} = 0.717 \pm 0.013(\text{stat}) \pm 0.008(\text{syst}), \quad (2)$$

$$C_{\psi K_S^0} = 0.008 \pm 0.012(\text{stat}) \pm 0.003(\text{syst}). \quad (3)$$

The graphical representation of the above results is depicted in Fig. 1 showing the time-dependent asymmetry.

According to the Standard Model the parameter $S_{\psi K_S^0}$ can be related to the CKM angle β as $S_{\psi K_S^0} = \sin(2\beta)$, up to suppressed contributions from penguin topologies to the decay amplitude [5]. The result of this analysis is more precise than the previous world average of this quantity [4].

3. Measurement of the CKM angle γ using the $B^\pm \rightarrow D^* h^\pm$ channels

This section describes briefly the determination of the CP -violating observables from $B^\pm \rightarrow D^* K^\pm$ and $B^\pm \rightarrow D^* \pi^\pm$ decays [6], where $D^*(D)$ is an admixture of D^{*0} and \overline{D}^{*0} (D^0 and \overline{D}^0)

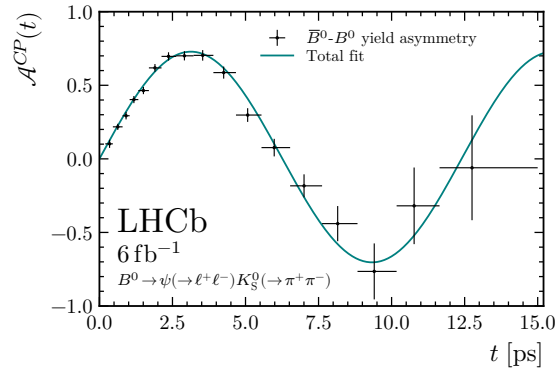


Figure 1: The figure presents the time-dependent CP asymmetry from the maximum-likelihood estimator of the binned asymmetry with the fit result overlaid. Figure from Ref. [5].

37 states and is reconstructed through the decay chains $D^* \rightarrow D\pi^0/\gamma$ and $D \rightarrow K_S^0\pi^+\pi^-/K_S^0K^+K^-$.
 38 The measurement has been performed by analysing the signal yield variation across the D decay
 39 phase space and is independent of any amplitude model. The data sample used was collected in
 40 pp collisions during Run 1-2. The CKM angle γ is determined to be $(69^{+13}_{-14})^\circ$ using the measured
 41 CP -violating observables. In the paper [6], the hadronic parameters $r_B^{D^*K^\pm}$, $r_B^{D^*\pi^\pm}$, $\delta_B^{D^*K^\pm}$, $\delta_B^{D^*\pi^\pm}$,
 42 which are the ratios and strong phase differences between favoured and suppressed B^\pm decays, are
 43 also reported. Here, the $r_B^{D^*K^\pm} - \gamma$ profile-likelihood plot showing 1σ and 2σ confidence regions
 44 for the subcombinations of decay modes is given in Fig. 2. These results are consistent with the
 world average [4].

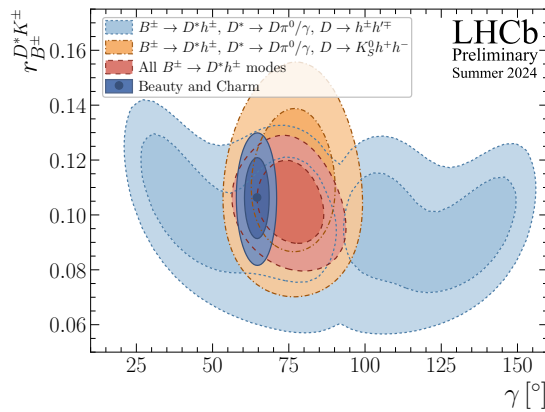


Figure 2: Profile-likelihood contours for the components that contribute towards the γ part of the combination, showing the breakdown of sensitivity among different subcombinations of decay modes. The data from full-reconstructed [6] and partially reconstructed [7] $B \rightarrow D^*h$ decays. The contours shown are the two-dimensional 1σ and 2σ contours, which correspond to the areas containing 68.3% and 95.4% of the distribution. Figure from [8].

46 **4. Measurement of the CKM angle γ in $B^\pm \rightarrow DK^*(892)^\pm$ decays.**

47 In this Section, the measurements of CP observables and the CKM angle γ in $B^\pm \rightarrow$
 48 $DK^*(892)^\pm$ decays are reported (see [9] for details). Here, D represents a superposition of
 49 D^0 and \bar{D}^0 states, The analysed sample includes data collected during Run 1 and Run 2. A
 50 comprehensive study of this channel has been performed with the D meson reconstructed in two-
 51 body final states $K^\pm\pi^\mp$, K^+K^- and $\pi^+\pi^-$; four-body final states $K^\pm\pi^\mp\pi^\pm\pi^\mp$ and $\pi^+\pi^-\pi^+\pi^-$; and
 52 three-body final states $K_S^0\pi^+\pi^-$ and $K_S^0K^+K^-$. This analysis includes the first observation of the
 53 suppressed $B^\pm \rightarrow [\pi^+K^-]_D K^{*\pm}$ and $B^\pm \rightarrow [\pi^+K^-\pi^+\pi^-]_D K^{*\pm}$ decays. The combined result gives
 54 $\gamma = (63 \pm 13)^\circ$ consistent with the world average [4]. The results are presented in Fig. 3 in the form
 of a profile-likelihood plot of the $r_B^{DK^*} - \gamma$ combination.

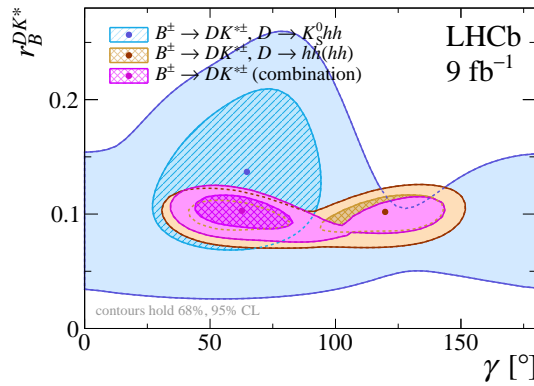


Figure 3: Two-dimensional scans $r_B^{D^0K^{*\pm}} - \gamma$ showing the contours evaluated with profile-likelihood method. Yellow, blue and magenta contours show the results for two- and four-body, three-body and all D-decay modes, respectively. The hatched and solid regions correspond to 68% and 95% confidence level, respectively. Figure from [9].

55

56 **5. Study of CP violation in $B^0 \rightarrow DK^*(892)^0$ decays with $D \rightarrow K\pi(\pi\pi), \pi\pi(\pi\pi),$** 57 **and KK final states**

58 CP -violating observables associated with the interference of $B^0 \rightarrow D^0K^*(892)^0$ and $B^0 \rightarrow$
 59 $D^0K^*(892)^0$ decay amplitudes have been measured. The following D^0 decay modes have been
 60 analysed $D^0 \rightarrow K^\mp\pi^\pm(\pi^+\pi^-)$, $D^0 \rightarrow \pi^+\pi^-(\pi^+\pi^-)$, and $D^0 \rightarrow K^+K^-$ using data collected during
 61 Run 1 and Run 2. The B^0 observables were used to constrain the parameter space of the CKM
 62 angle γ and the hadronic parameters $r_{B^0}^{DK^*}$ and $\delta_{B^0}^{DK^*}$ with inputs from other measurements. In a
 63 combined analysis, these measurements allow for four solutions in the parameter space, only one of
 64 which is consistent with the world average. The outcome in the form of a two-dimensional $r_{B^0}^{DK^*} - \gamma$
 65 profile-likelihood is presented in Fig. 4 showing the results the analysis where D meson decays into
 66 two or four charged hadrons [10] (left panel), together with the same results combined with the
 67 analysis where D decays into $K_S^0h^+h^-$ (right panel).

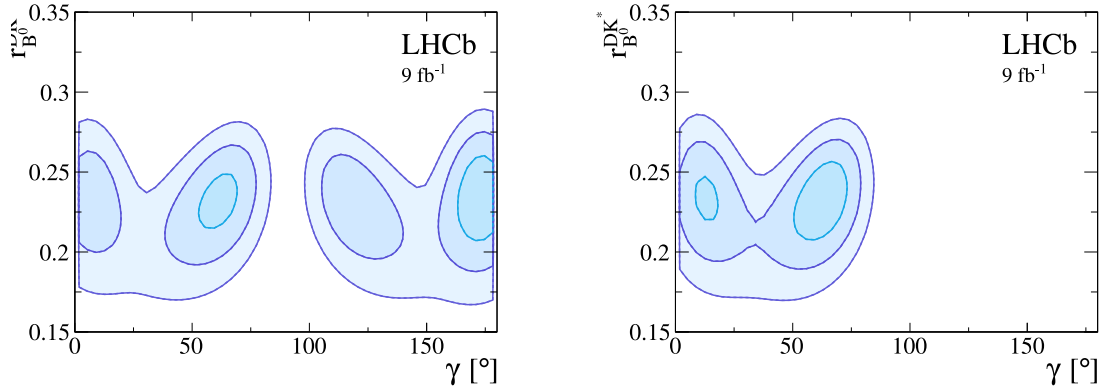


Figure 4: Confidence level contours from a profile-likelihood analysis of the B^0 -related CP -violating observables from (left) just the analysis [10] and (right) combined with the results from Ref. [11] (with $D \rightarrow K_S^0 h^+ h^-$) projected to the $\gamma - r_{B^0}^{DK^*}$ plane. Contours contain 68.3%, 95.4%, and 99.7% of the distribution. Figure from [10].

68 6. Search for CP violation in $D^+ \rightarrow K^- K^+ \pi^+$

69 A search for violation of the CP symmetry in the $D^+ \rightarrow K^- K^+ \pi^+$ decay is enabled by a
 70 novel model-independent technique comparing the D^+ and D^- phase-space distributions, with
 71 instrumental asymmetries subtracted using the $D_s^+ \rightarrow K^- K^+ \pi^+$ decay as a control channel. The
 72 analysis [12] exploits the pp collision data corresponding to an integrated luminosity of 5.4 fb^{-1}
 73 (a subset of Run 2). The p -value for the hypothesis of CP conservation is 8.1%.

74 The CP observables $A_{CP|S}^{\phi\pi^+} = (0.95 \pm 0.43\text{stat} \pm 0.26\text{syst}) \times 10^{-3}$ and $A_{CP|S}^{K^*0 K^+} = (-0.26 \pm$
 75 $0.56\text{stat} \pm 0.18\text{syst}) \times 10^{-3}$ are also measured. These results show no evidence of CP violation
 76 and represent the most sensitive search performed through the phase space of a multi-body decay.
 77 The Dalitz plot for the signal and control channel with the binning scheme overlaid is presented in
 Fig. 5.

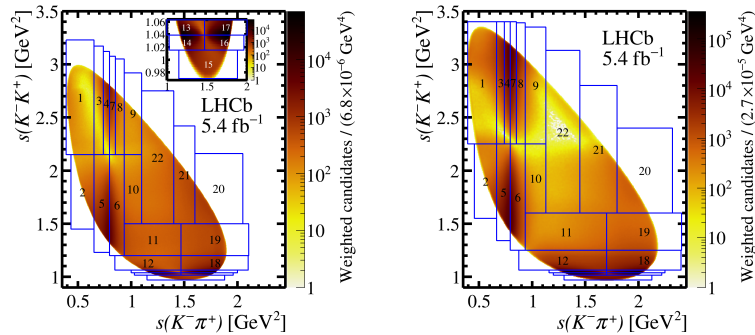


Figure 5: Dalitz plots for (left) $D^+ \rightarrow K^- K^+ \pi^+$ and (right) $D_s^+ \rightarrow K^- K^+ \pi^+$ decays in data with the binning scheme overlaid. The enlarged inset shows the bins around the $\phi\pi^+$ region, where the same numbering scheme is followed for both channels. Figure from [12].

7. Evidence for direct CP -violation in baryons

A study of Λ_b^0 and Ξ_b^0 decays to $\Lambda h^+ h'^- (h(\prime) = \pi, K)$ has been performed using pp collision data collected during LHC Runs 1–2. The analysis exploits the branching fraction of the $\Lambda_b^0 \rightarrow \Lambda_c^+(\rightarrow \Lambda\pi^+)\pi^-$ decay as control channel and the decays $\Lambda_b^0 \rightarrow \Lambda\pi^+\pi^-$ and $\Xi_b^0 \rightarrow \Lambda K^-\pi^+$. For decay modes with sufficient signal yields, CP asymmetries are measured in the full and localised regions of the final-state phase space. To reduce systematic uncertainties, the difference between the CP asymmetry of each signal decay and the $\Lambda_b^0 \rightarrow \Lambda_c^+(\Lambda\pi^+)\pi^-$ decay, ΔA_{CP} , is measured. Assuming there is no CP violation for the control mode, valid within the experimental uncertainties of this analysis, ΔA_{CP} gives the measurement of the CP asymmetry for the signal decay. Evidence of CPV of the level of 3.1σ is found for CP violation in the $\Lambda_b^0 \rightarrow \Lambda K^+ K^-$ decay:

$$\Delta A^{CP}(\Lambda_b^0 \rightarrow \Lambda K^+ K^-) = 0.083 \pm 0.023 \pm 0.016. \quad (4)$$

Fig. 6 compares the fit results to the $\Lambda K^+ K^-$ and $\bar{\Lambda} K^+ K^-$ invariant-mass spectra: a clear difference in signal yields between Λ_b^0 and $\bar{\Lambda}_b^0$ decays can be seen. It is interpreted as originating primarily from an asymmetric $\Lambda_b^0 \rightarrow N^{*+} K^-$ decay amplitude. The measured CP asymmetries for the other decays are compatible with zero.

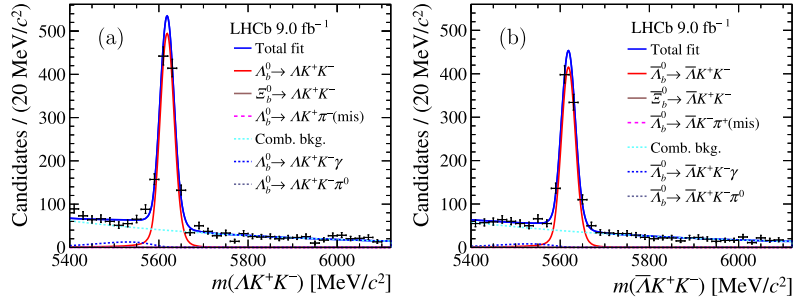


Figure 6: Mass distributions of (a) $\Lambda_b^0 \rightarrow \Lambda K^+ K^-$ and (b) $\bar{\Lambda}_b^0 \rightarrow \bar{\Lambda} K^+ K^-$ decays, with the fit projections. Figure from [13].

92

8. First evidence for direct CP violation in beauty to charmonium decays

The CP asymmetry and branching fraction of the CKM-suppressed decay $B^+ \rightarrow J/\psi\pi^+$ are precisely measured relative to the favoured decay $B^+ \rightarrow J/\psi K^+$, using a sample of pp collision data corresponding to an integrated luminosity of 5.4 fb^{-1} recorded at center-of-mass energy of 13 TeV (for details see [14]). The results of the CP asymmetry difference and branching fraction ratio read

$$\Delta A^{CP} \equiv A^{CP}(B^+ \rightarrow J/\psi\pi^+) - A^{CP}(B^+ \rightarrow J/\psi K^+) = (1.29 \pm 0.49 \pm 0.08) \times 10^{-2}, \quad (5)$$

$$R_{\pi/K} \equiv \frac{\mathcal{B}(B^+ \rightarrow J/\psi\pi^+)}{\mathcal{B}(B^+ \rightarrow J/\psi K^+)} = (3.852 \pm 0.022 \pm 0.018) \times 10^{-2}, \quad (6)$$

where the first uncertainties are statistical and the second systematic. A combination with previous LHCb results based on data collected at 7 and 8 TeV in 2011 and 2012 yields $\Delta A^{CP} = (1.42 \pm$

100

101 $0.43 \pm 0.08) \times 10^{-2}$ and $R_{\pi/K} = (3.846 \pm 0.018 \pm 0.018) \times 10^{-2}$. The combined ΔA^{CP} value
 102 deviates from zero by 3.2 standard deviations, providing the first evidence for direct CP violation
 103 in the amplitudes of beauty decays to charmonium final states.

104 References

- 105 [1] LHCb collaboration, *The LHCb Detector at the LHC*, *JINST* **3** (2008) S08005.
- 106 [2] LHCb collaboration, *LHCb Detector Performance*, *Int. J. Mod. Phys. A* **30** (2015) 1530022
 107 [1412.6352].
- 108 [3] PARTICLE DATA GROUP collaboration, *Review of Particle Physics; Chapter 13: CP violation in*
 109 *the quark sector*, *Progress of Theoretical and Experimental Physics* **2022** (2022) 083C01
 110 [<https://academic.oup.com/ptep/article-pdf/2022/8/083C01/49175539/ptac097.pdf>].
- 111 [4] HFLAV collaboration, *Averages of b-hadron, c-hadron, and τ -lepton properties as of 2021*,
 112 *Phys. Rev. D* **107** (2023) 052008 [2206.07501].
- 113 [5] LHCb collaboration, *Measurement of CP Violation in $B^0 \rightarrow \psi(\rightarrow \ell^+\ell^-)K_S^0(\rightarrow \pi^+\pi^-)$*
 114 *Decays*, *Phys. Rev. Lett.* **132** (2024) 021801 [2309.09728].
- 115 [6] LHCb collaboration, *Measurement of the CKM angle γ using the $B^\pm \rightarrow D^*h^\pm$ channels*,
 116 *JHEP* **12** (2023) 013 [2310.04277].
- 117 [7] LHCb collaboration, *A model-independent measurement of the CKM angle γ in partially*
 118 *reconstructed $B^\pm \rightarrow D^*h^\pm$ decays with $D \rightarrow K_S^0h^+h^-$ ($h = \pi, K$)*, *JHEP* **02** (2024) 118
 119 [2311.10434].
- 120 [8] LHCb collaboration, *Simultaneous determination of the CKM angle γ and parameters*
 121 *related to mixing and CP violation in the charm sector*, 2024. 10.17181/CERN.8CUC.W3FT.
- 122 [9] LHCb collaboration, *Measurement of the CKM angle γ in $B^\pm \rightarrow DK^*(892)^\pm$ decays*, *JHEP*
 123 **02** (2025) 113 [2410.21115].
- 124 [10] LHCb collaboration, *Study of CP violation in $B^0 \rightarrow DK^*(892)^0$ decays with $D \rightarrow K\pi(\pi\pi)$,*
 125 *$\pi\pi(\pi\pi)$, and KK final states*, *JHEP* **05** (2024) 025 [2401.17934].
- 126 [11] LHCb collaboration, *Measurement of the CKM angle γ in the $B^0 \rightarrow DK^{*0}$ channel using*
 127 *self-conjugate $D \rightarrow K_S^0h^+h^-$ decays*, *Eur. Phys. J. C* **84** (2024) 206 [2309.05514].
- 128 [12] LHCb collaboration, *Measurement of CP Violation Observables in $D^+ \rightarrow K^-K^+\pi^+$ Decays*,
 129 *Phys. Rev. Lett.* **133** (2024) 251801 [2409.01414].
- 130 [13] LHCb collaboration, *Study of Λ_b^0 and Ξ_b^0 decays to Λh^+h^- and evidence for CP violation in*
 131 *$\Lambda_b^0 \rightarrow \Lambda K^+K^-$ decays*, 2411.15441.
- 132 [14] LHCb collaboration, *First evidence for direct CP violation in beauty to charmonium decays*,
 133 2411.12178.